Egypt.J.Chem. **Vol. 62**, No. 9. pp. 1575 - 1585 (2019)

Egyptian Journal of Chemistry
http://ejchem.journals.ekb.eg/

Effect of Cadmium Sulfide Quantum Dots Prepared by Chemical Bath Deposition Technique on the Performance of Solar Cell

Z. Abdel Hamid[*1], H. B. Hassan[2], Manal A. Hassan[1], M. Hussein Mourad[3], S. Anwar[1]

[1]*Central Metallurgical Research and Development Institute, Helwan, Cairo, Egypt.*
[2]*Faculty of Science, Cairo University, Giza, Egypt.*
[3]*National Institute of Laser Enhanced Sciences, Engineering Department, Cairo University, Egypt.*

QUANTUM dots are very tiny semiconductor particles used in solar cells; their optical and electronic properties differ from those of macro particles. They could improve the performance of solar cells if they are prepared in the suitable size. In this work, cadmium sulfide (CdS) quantum dot (QD) thin films were prepared on transparent conductive fluorine-doped tin oxide substrates. The formation and deposition of CdS QDs were optimized using the chemical bath deposition method under varied operating conditions (precursor concentration, and temperature). Chemical bath deposition is an effective method for the deposition of CdS on porous TiO_2 films as QDs. The structural, morphological, and optical properties of the prepared CdS thin films were studied using X-ray diffraction, field-emission scanning electron microscopy, Raman spectroscopy and UV-Vis-near infrared spectroscopy. The particle size of the CdS QDs was calculated to be 3–7 nm from the observed X-ray diffraction pattern. The band gap was blue shifted in the UV-Vis absorption spectrum compared with that of bulk CdS, confirming the formation of CdSQDs.

Keywords: Semiconductors, Quantum dots, Chemical bath deposition, TiO_2, CdS, Solar cells.

Introduction

Solar energy is one of the cleanest and most abundant renewable energy sources on the earth surface. The sunlight can be directly converted to electricity using solar cells. Improving the materials that constitute the solar cells especially the photoanodes will increase the performance of the solar cells and increase its efficiency. Confining the dimensions of a material to the nanometer scale imposes limits on motion or the kinetic energy of that material, giving rise to quantization of electron and hole energies [1]. This leads to the need for higher energies to separate the charges in semiconductor particles compared with those in the bulk. Decreasing the particle size introduces such 3D confinement and varies the material properties, such as the optical bandgap, photoluminescence, extinction coefficient and energy transfer, away from those of the bulk material [2]. Semiconductor nanoparticles with theoretical 0D structures, in which the motion of conduction-band electrons and valence-band holes are confined in all three spatial directions, are referred to as quantum dots (QDs) [2]. In recent years, many QD materials have been investigated as sensitizers to replace the organic dyes of dye-sensitized solar cells (DSSCs). For such applications, termed QD-sensitized solar cells (QDSSCs), QDs are loaded onto the surface of nanostructured porous films formed on a transparent conductive oxide surface [3]. Semiconductor materials such as CdS, CdSe, CdTe, PbS, PbSe, InP, HgTe, Ag_2S, Sb_2S_3, Bi_2S_3 Cu_2S, and $CuInS_2$ have been used for many applications concerning sensitized solar cells [4]; however, CdSQDs in particular have suitable properties to realize good efficiency in QDSSCs [4]. CdS is one of the most important II–VI semiconductor compounds because it has excellent optical properties. Therefore, great efforts have been made to synthesize and study

*Corresponding author e-mail: forzeinab@yahoo.com
Received 4/12/2018; Accepted 19/3/2019
DOI: 10.21608/ejchem.2019.6509.1547

the optical properties of CdS-related nanoparticles and quantum dots [5-6].

The energy levels of the charges (electrons and holes) were found to be the main factor affecting the behavior of the QD materials. Some useful properties of QDs are their ability to generate multiple excitons, photostability, and high absorption coefficient, which are known to decrease the dark current and increase the efficiency of a solar cell. Furthermore, QD materials have tunable band gap energy levels, offering opportunities to improve their light-harvesting ability that could improve the efficiency of solar cells [6].

Several routes have been used to fabricate CdSQDs [7]. Generally, top-down processing or bottom-up approaches are used for CdS QD synthesis. Top-down methods include molecular-beam epitaxy, ion implantation, electron-beam lithography, and X-ray lithography [8-11]. Different self-assembly (bottom-up) techniques have been used to synthesize CdSQDs, and these approaches can be divided into wet chemistry and vapor-phase methods [12]. Wet chemistry methods include sol–gel techniques [13, 14], competitive reaction chemistry, hot-solution decomposition [15], sonic wave or microwave reactions [16], and electrochemistry. Vapor-phase methods begin with the formation of layers through an atom-by-atom process.

In this work, CdS QDs were deposited by a wet chemistry method called chemical bath deposition (CBD) because it is a simple and low cost process. It is an in-situ method that uses a single precursor solution for QD material deposition [17]. The precursor solution in this case contained both the cations and anions to be deposited on a fluoride-doped tin oxide (FTO) substrate. The solution pH and temperature were carefully controlled in order to optimize the CBD in terms of layer stability and nanoparticle size. The prepared QDs were characterized using (XRD), electron microscopy, Raman spectroscopy, and UV-Vis-NIR spectroscopy to identify the structure and morphology and to estimate the band gap energy. QDSSC electrodes were fabricated using the prepared CdS QDs loaded on the surface of TiO_2.

Experimental

Materials

Cadmium sulfate ($CdSO_4 \cdot 8H_2O$, 99%, VEB Laborchemie Apolda GmbH, Germany), thiourea ($CS(NH_2)_2$, Loba Chemie, India), 28 % NH_4OH (Koch-Light Laboratories Ltd, UK), triethanolamine, sodium hydroxide (NaOH, Koch-Light Laboratories Ltd), titanium(IV) isopropoxide (97%, Sigma–Aldrich), glacial acetic acid, concentrated nitric acid (Sigma–Aldrich), citric acid (Sigma–Aldrich), Triton X-100, 10 Ω FTO glass substrates (thickness 1.1 mm, coating thickness 150 nm), and Teflon-lined stainless autoclave tubes were used as received.

Preparation of anatase TiO_2

AnataseTiO_2 (P25) powder was prepared from titanium(IV) isopropoxide (27 g) and glacial acetic acid (5.53 g). Then, deionized water (133 ml) was added, and the solution was stirred for 1 h. After stirring, concentrated nitric acid (1.82 ml) was added, and the temperature was increased to 80 °C and kept constant for 2 h until a milky white solution was obtained. The volume of the solution was increased to 165 ml using deionized water, and then, the solution was kept in an oven at 250°C for 12 h by using a Teflon-lined stainless-steel autoclave. The pure P25 anatase TiO_2 was isolated by centrifugation(2 h) and washed several times with deionized water and then dried at 50 °C [18].

Preparation of mesoporous TiO_2 films

FTO glass samples were cleaned successively using sodium dodecyl sulfate and then sequentially sonicated in deionized water, ethanol, acetone and finally isopropanol for 30 min. for each reagent, respectively. The substrates were dried at 140°C for 15 min. prior to the deposition process. A paste of TiO_2 was prepared by mixing P25 anatase TiO_2 powder (1 g), citric acid (1 ml) and one drop of Triton X-100. Transparent TiO_2mesoporous films were prepared by doctor blading (C.B.G theTiO_2 paste on to the cleaned FTO glass substrates. The films were then sintered at 500°C in inert atmosphere for 30 min. to decrease the impurities and enhance the crystallinity.

Growth of CdS QD layers using CBD

Different concentrations of $CdSO_4$ and thiourea were tested (Table 1) to study the effect of changing the concentration on the composition of the resulting CdS QD films. NH_4OH (28% solution) was added dropwise into a 100 ml beaker containing $CdSO_4$ solution (0.05–0.2 M and 25 ml) until the initially formed white precipitate was completely dissolved. The substrates were fixed vertically in the bath. Then, $CS(NH_2)_2$ (0.1 or 0.2M and 25 ml) was poured into the beaker. Finally, distilled water was gradually added to

increase the volume to 100 ml. The deposition process for all samples was performed at 25–70 °C on a hot plate under magnetic stirring. Stirring was continued for 10 min., dried using air blower, then the samples were stored in desiccators. (Fig. 1).

TABLE 1. Chemical compositions and operating conditions* for CdS deposition.

Sample no.	$CdSO_4$ conc (M)	$(CS(NH_2)_2)$ conc(M)	Temp. (°C)
4	0.05	0.1	70
8	0.1	0.1	70
5	0.15	0.1	70
6	0.2	0.1	70
3	0.2	0.2	70
1	0.2	0.2	25
2	0.2	0.2	45
7	0.2	0.2	55

*Time of deposition was 10 minutes for all samples.

Material characterization

Field-emission scanning electron microscopy (FE-SEM) was performed on a Quanta FEG microscope (FEI, the Netherlands). High-resolution transmission electron microscopy (HR-TEM) images of TiO_2 and CdS QDs were obtained using an FEI Tecnai G2 20S-Twin microscope with an accelerating voltage of 200 kV. Raman spectra were obtained using a Sentera spectrometer (Bruker, Germany) with a laser wavelength of 532 nm (doubled Nd:YAG laser) and a power of 3 mW. The spectra were recorded over the range of 1200–100 cm^{-1}. UV-Vis-NIR absorption spectra were recorded using a Jasco V-570 UV-Vis-NIR scanning spectrophotometer. XRD data were obtained using a Bruker AXSD8 Advanced diffractometer with a CuKα radiation source (λ= 1.54056 Å) operating at 40 kV and 40 mA. The diffraction data were recorded for 2θ values between 10° and 80°.

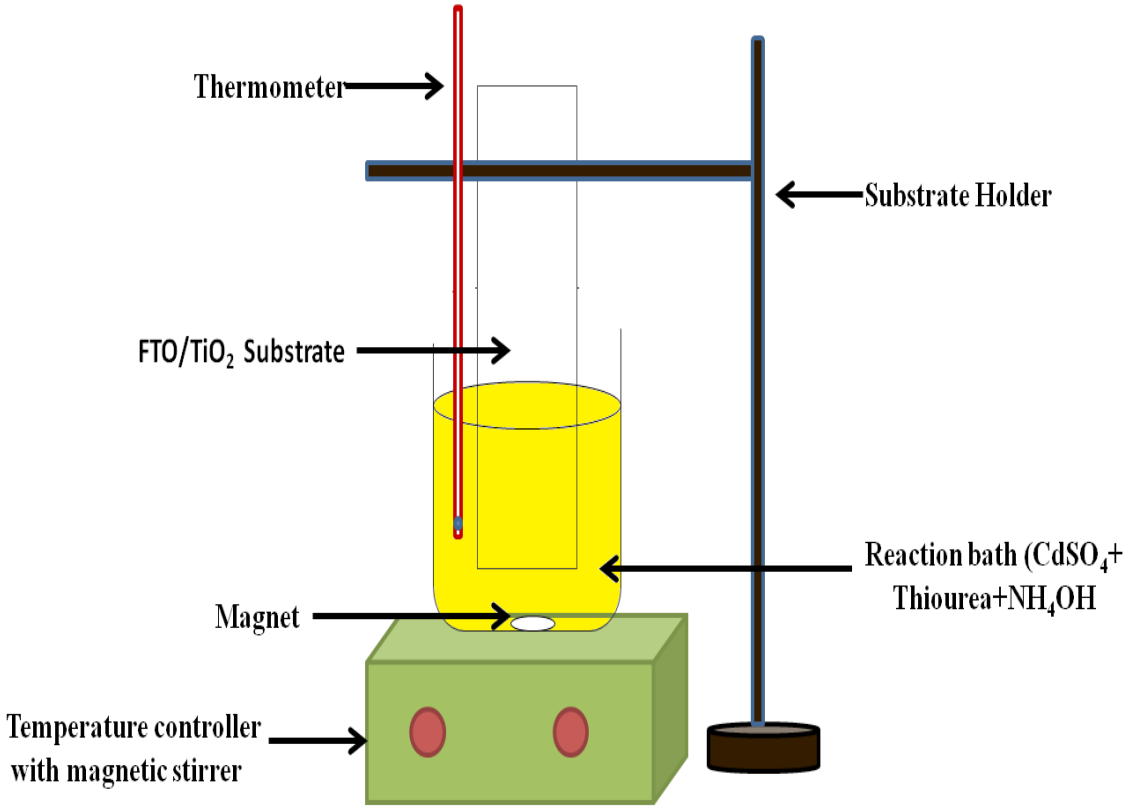

Fig. 1. Schematic diagram representing the CBD technique.

Results and Discussion

Recently, deposition of metal oxide layers with quantum dots (QDs) has drawn considerable attention for enhancing photovoltaic devices. The composition and phase purity of the prepared TiO_2 nanoparticles were estimated by XRD. Figure 2 illustrates a typical XRD pattern of a thin film of TiO_2 prepared in this study. The diffraction peaks at 25.4°, 37.2° , 48.5° , 54.1°, 55.7°, and 63.2° corresponding to the (101), (112), (200), (105), (211) and (204) phases of TiO_2, respectively, were observed according to the standard pattern (JCPDS No: 88-1175 and 84-1286). The absence of broad peaks indicates the sample is crystallographically pure. The sharp high-intensity peaks observed at 25.4° and 48.5° indicate the formation of TiO_2 in the anatase phase [19]. From the XRD pattern, the average crystal size of the TiO_2 nanoparticles was 7.23 nm, as calculated using the Scherrer formula (1) [20]:

$$D\rho = \frac{0.94\,\lambda}{\beta \cos\theta} \quad (1)$$

Where $\lambda$is the wavelength of the X-rays, β is the full width at half-maximum (FWHM), θ is the diffraction angle, and D_p is the crystal size.

The particle size and crystallinity of the TiO_2 powder were investigated by HR-TEM, and the acquired images confirmed the results of the XRD study (Fig. 3a). The TiO_2 nanoparticles had a mostly spherical morphology and were in the anatase phase. Figure 3(b &c) shows FE-SEM images of the nano-TiO_2 thin film (prepared by doctor blading) at different magnifications. The images illustrate that the TiO_2 particles were porous and spherical with a smooth surface. In addition, the size of the particles was approximately 18–22 nm.

Films of CdS were fabricated on the anatase TiO_2 thin films pre-loaded onto FTO glass in an alkaline chemical bath solution. The deposition was carried out according to the following proposed reaction mechanism in which $CdSO_4$ is the source of Cd^{2+} ions and thiourea supplies S^{2-} ions through a hydrolytic process in an alkaline medium [21] [Eqs. 2–8)]:

$$Cd^{2+} + 4NH_3 \longrightarrow [Cd(NH_3)_4]^{2+} \quad (2)$$

$$[Cd(NH_3)_4]^{2+} \longrightarrow Cd^{2+} + 4NH_3 \quad (3)$$

$$NH_3 + H_2O \longrightarrow NH_4^{2+} + OH^- \quad (4)$$

$$Cd^{2+} + 2OH^- \longrightarrow Cd(OH)_2 \quad (5)$$

$$CS(NH_2)_2 + 2OH^- \longrightarrow [HS^+] + H_2O + CH_2N \quad (6)$$

$$[HS]^+ + OH^- \longrightarrow S^{2-} + H_2O \quad (7)$$

$$[Cd(NH_3)_4]^{2+} + S^{2-} \longrightarrow CdS + NH_3 \quad (8)$$

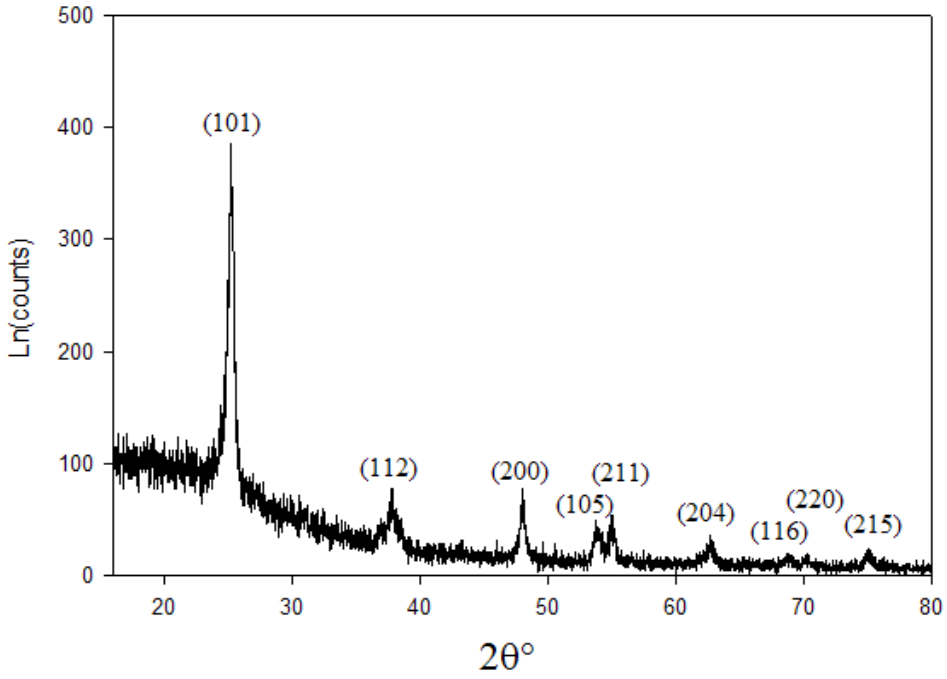

Fig. 2. XRD pattern of an anatase TiO_2 thin film formed using the doctor blade method.

The morphological, structural and optical properties of these films were studied. The results revealed that the fabricated thin films were tightly adhered (Scratch test ISO- 2409 class zero) to the substrates, homogeneous, smooth, reflective, and light yellow in color. The structures of the CdS–TiO_2 films were analyzed using X-ray diffraction. Figure 4 shows the X-ray diffraction pattern for a CdS film on a TiO_2 layer, and the most important peaks appeared at 2θ values of 26.67, 44.63°, and 51.41°, indicating preferred orientations of (111), (220), and (311), respectively, for the CdS QDs. The diffraction peaks at 2θ values of 25.4° and 51.4° correspond to TiO_2, and those at 2θ values of 33.5°, 38.1°, and 61.6° correspond to FTO. The average grain size of the CdS QDs, as calculated by the Scherrer formula, was approximately 3.92 nm. The surface morphologies of the CdS films were observed by FE-SEM (Fig. 3d). The images revealed that the surface consisted of spherical grains with sizes of 15–24 nm and had a smooth appearance. The fine grains are formed due to the homogeneous nucleation of CdS particles on the surface. The shape and grain size of CdS films greatly affect the electrical properties of the resulting solar cells [22].

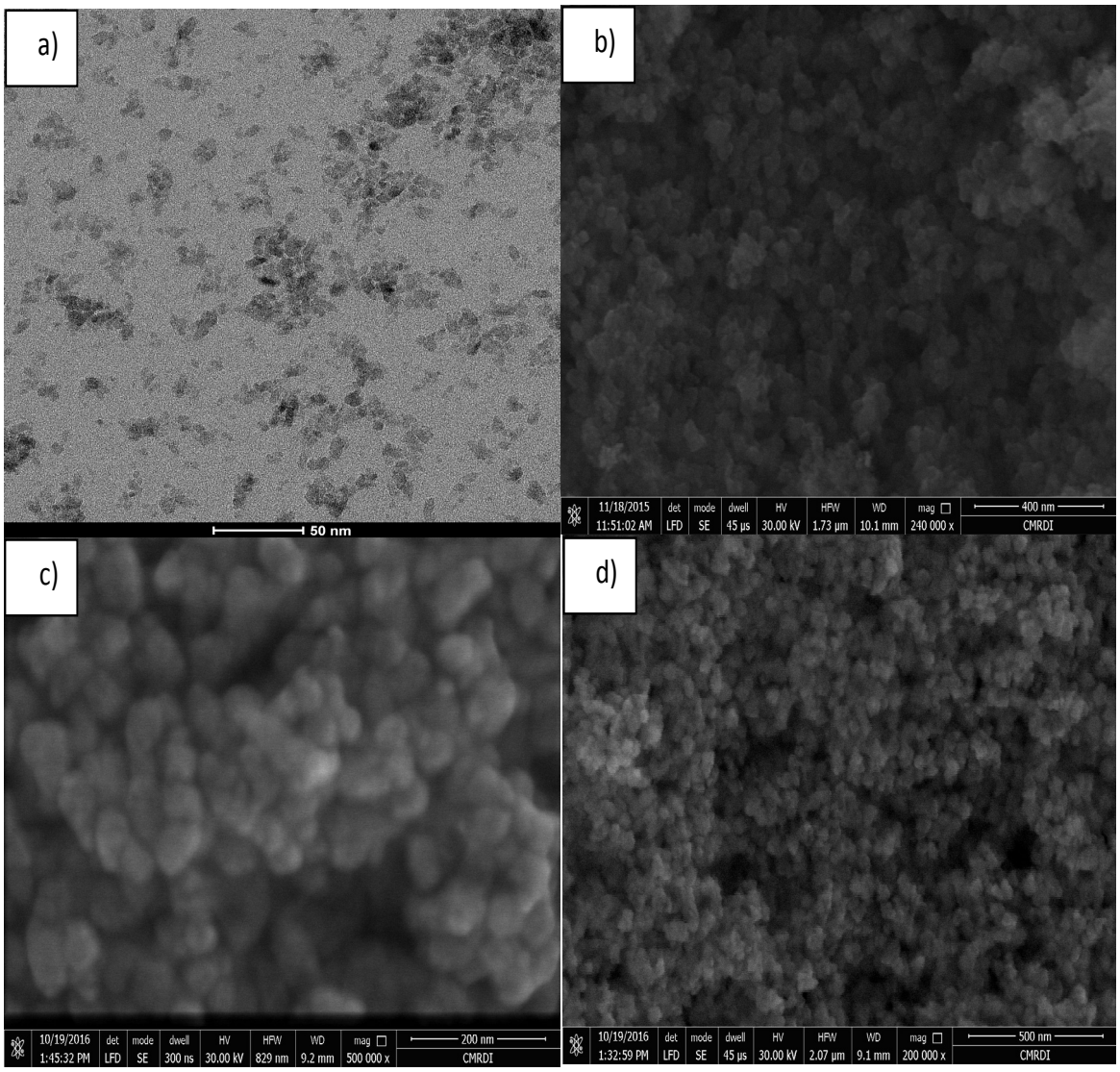

Fig. 3. a) HR-TEM image of TiO_2 nano particles as prepared.
b&c) FE-SEM images of nanostructure anatase TiO_2 prepared using the doctor blade method at different magnifications.
d) FE-SEM images of the CdS QD layer prepared from a solution containing 0.2 M $CdSO_4$ and 0.2 M thiourea operated at 70 °C and 10 min.

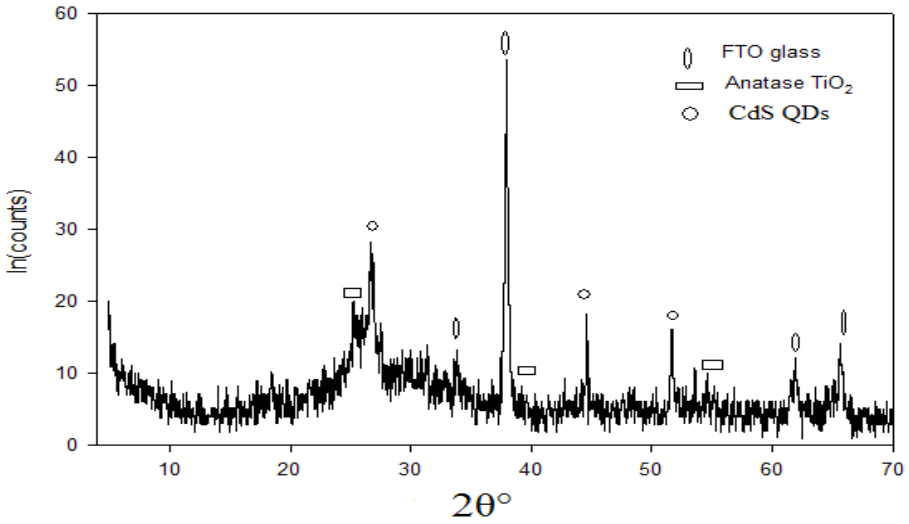

Fig. 4. XRD pattern of the CdS QD / anatase TiO_2 thin film on FTO at 70 °C with concentration of 0.2 M for both $CdSO_4$ and $CS(NH_2)_2$.

UV-Visible spectrometry was used for measurement the ability of photoanode to absorb light for solar cell applications. The UV-Vis absorption spectrum of the CdS–TiO_2 photoelectrode is shown in Fig. 5a. The absorption peak of the CdS thin films was located at 493 nm, whereas the absorption edge of bulk CdS was blue shifted to 515 nm as a result of the decrease in the average size of CdS particles (3.92 nm). Thus, the co-sensitizing effect of CdS can enhance the performance of the QDSSC [23]. Furthermore, the band gaps of the grown CdS thin films were calculated from the following equation [24,25]:

$$\alpha = A(h\nu - E_g)^m / h\nu \qquad (9)$$

Where α is the absorption coefficient, E_g is the optical band gap, A is a constant which refer to the effective mass associated with the band, and $m$is 1/2 for a direct-gap material, while the value of m is 2 for an indirect-gap material and 3/2 for a forbidden direct energy gap. The energy gap (Fig. 5b) was estimated by extrapolating the straight line of $(\alpha h\nu)^2$ plotted as a function of the photon energy of the sample. A linear relation between $(\alpha h\nu)^2$ and $h\nu$ indicates a direct band gap, which was 2.63 eV, whereas the band gap of bulk CdSwas 2.42eV. The increase in the band gap might be due to the quantum confinement effect in QDs (as the crystal size decreases, the band gap increases).

Raman spectroscopy was performed on the CdS-deposited photoanode to confirm the formation of the CdS. The Raman peaks at 299 and 600 cm^{-1} increased in intensity for QDs deposited at increasing temperature, because the layers deposited were thicker. Figure 5c shows CdS QDs formed at 70 °C. The reported peaks for bulk CdS are located at 305 and 605 cm^{-1}. The shift we observed in the CdS peaks is consistent with the spatial phonon confinement effect for QDs [25–27]. For hexagonal CdS, the first-order Raman band at 299 cm^{-1} and the second-order band at 600 cm^{-1} correspond to the first-order (1LO) and second-order (2LO) vibrations of hexagonal CdS, respectively. Here, LO refers to longitudinal optical phonons that polarize along the *z* direction parallel to the unit cell edge. The 1LO frequency of bulk CdS is known to be 305 cm^{-1}. The 2LO mode can be understood as a resonant Raman effect due to the limited size of the CdS particles or as transitions from the cluster system [26-28].

To evaluate the photovoltaic performance of CdS–TiO_2, QDSSCs were fabricated, and the resulting current density–voltage (*J–V*) curves were obtained (Fig. 6 and Table 2). Table 2 gives the performance of QDSSCs fabricated with CdS–TiO_2 prepared under different operating conditions, in terms of the open-circuit potential (V_{OC}), short-circuit current density (J_{SC}), fill factor (ff), and total energy conversion efficiency (η). Figure 6 shows a comparison of the photovoltaic *J–V* performance of the QDSSCs under 1 sun illumination using a Cu_2S–brass counter electrode and polysulfide electrolyte [29].

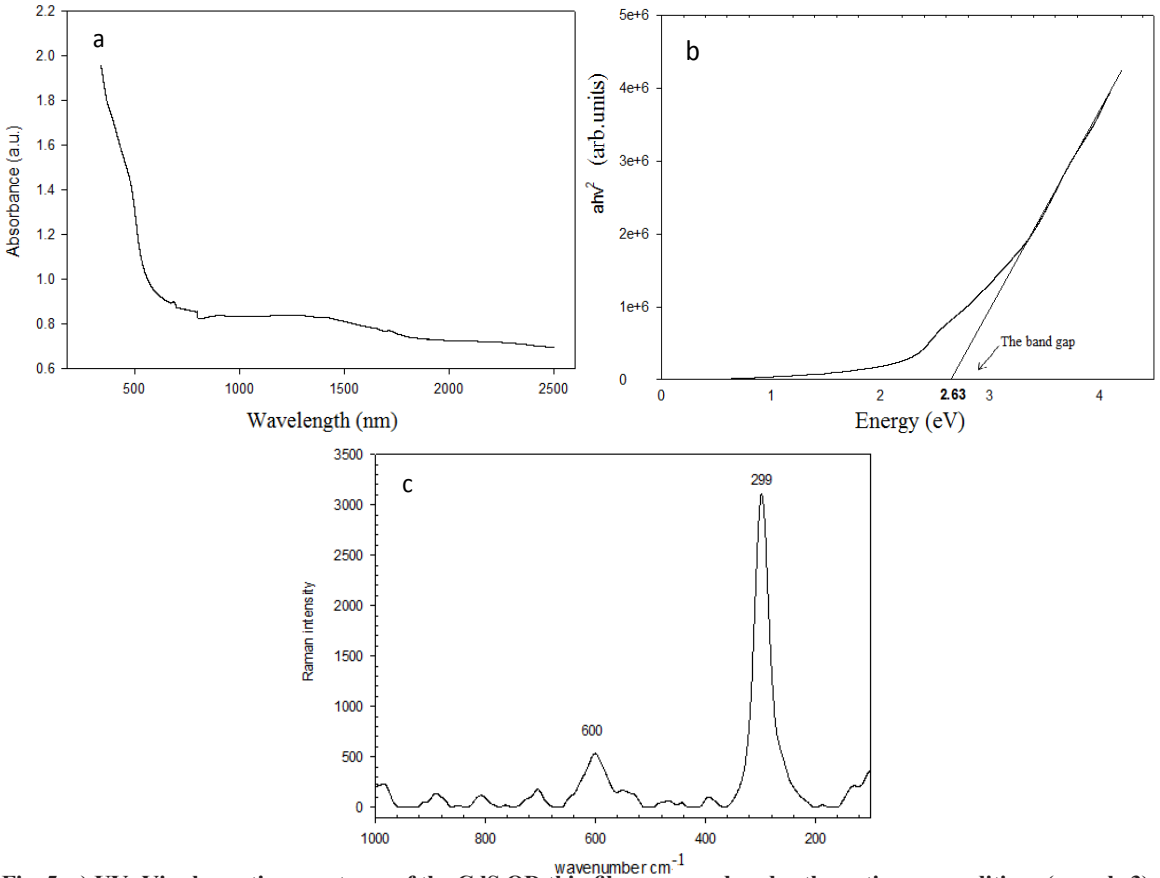

Fig. 5. a) UV- Vis absorption spectrum of the CdS QD thin film prepared under the optimum conditions (sample 3).
b) The band gap of the grown CdS QD thin film (sample 3).
c) Raman spectrum of the CdS QD-deposited photoanode (sample 3).

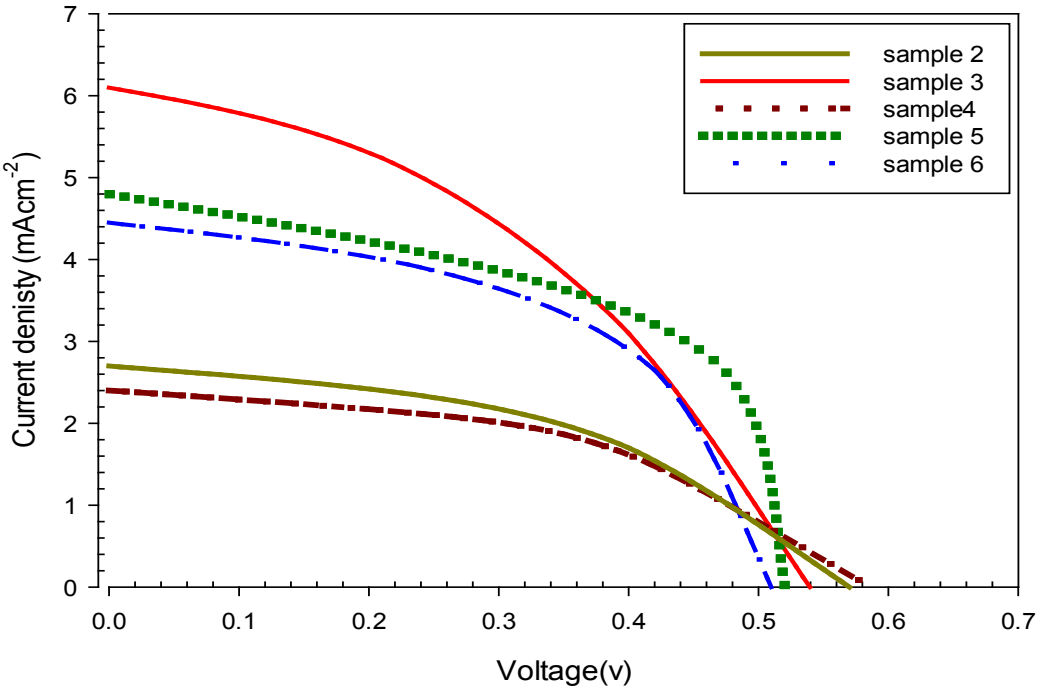

Fig. 6. J–V curves of QDSCs with CdS QD/TiO_2 electrodes fabricated under different operating conditions.

TABLE 2. Cell efficiency and ff with CdS QD/TiO_2 electrodes fabricated at different operating conditions.

Sample no.	$CdSO_4$ conc (M)	$CS(NH_2)_2$ conc (M)	Temp (°C)	Voc (V)	ISC (mA cm^{-2})	ff	Ŋ (%)
2	0.2	0.2	45	0.57	2.71	0.454	0.699
3	0.2	0.2	70	0.54	6.10	0.417	1.367
4	0.05	0.1	70	0.59	2.400	0.463	0.651
5	0.15	0.1	70	0.52	4.800	0.581	1.345
6	0.2	0.1	70	0.51	4.450	0.516	1.172

The mechanism of photoelectrons generation can be explained as the following reactions [30]:

$$CdS + h\upsilon CdS \longrightarrow (e^- + h^+) \quad (10)$$

$$CdS\,(e^- + h^+) + TiO_2 \longrightarrow CdS\,(h^+) + TiO_2\,(e^-) \quad (11)$$

$$TiO_2\,(e^-) \longrightarrow \text{Photocurrent} \quad (12)$$

The process is carried when sunlight falls on the cell surface and absorbed by cadmium sulfide quantum dots molecules which will produce photoelectrons as shown in the first reaction. The resulted electrons are rapidly injected into the conduction band of TiO_2 which will generate a photocurrent. The holes which left in CdS QDs will be compensated by the polysulfide electrolyte in the cell.

It can be seen that increasing bath temperature (keeping the deposition time constant at 10 min) leads to increase in the overall energy conversion cell efficiency. The CdS QDs formed a good adhesive layer at 70 °C, whereas if the temperature was decreased to 45 °C, the efficiency decreased from 1.367 to 0.699. The significantly improved cell performance (1.367%) of the QDSSC with CdS QDs formed at 70°C was largely due to the increased J_{SC}. This might be due to the increased number of electrons injected into TiO_2 resulting from the increased number of assembled QDs; this would result in enhanced light absorption. The overall efficiency of the QDSSC decreased as the concentration of the cadmium precursor and/or the sulfur precursor was decreased, due to the low coverage of the cell with layers of CdS.

The efficiency of the prepared CdS QDSSC is acceptable compared with other results obtained with the CBD method, as shown in Table 3.

TABLE 3. Efficiency of CdS QDs deposited using CBD: a comparison between this work and selected published results of others.

Efficiency (%)	Reference
1.5	[31]
1.35	[32]
2.13	[33]
1.09	[34]
1.08	[35]
1.37	this work

Conclusion

Thin films of CdSQDs were successfully prepared through a simple, low-cost, and more efficient CBD method. The deposition of QDs was optimized by varying the operating conditions (precursor concentration and temperature). From the XRD results the average particle size was 3.92 nm, and the particles were spherical. The optical properties showed a blue shift due to the nanoscale size of the CdS thin films, which is in agreement with the grain size determined by the XRD study. The optical band gap energy (E_g) of the CdS QDs was determined from UV spectroscopic data to be 2.63 eV. Excellent performance, with η of 1.367%, V_{OC} of 0.539 V, J_{SC} of 6.100 mA cm^{-2}, and ff of 0.417, was obtained for CdS–TiO_2 QDSSCs fabricated at high temperature (70°C) with higher Cd and S precursor concentrations.

Acknowledgements

This study was performed through scientific cooperation between Central Metallurgical R&D Institute (CMRDI), Egypt and Academy of Scientific Research &Technology (ASRT), scientists for next generation (SNG) scholarship, EGYPT.

References

1. Mahmoud F.A., Assem Y., Shehata A.B., Motaung D.E. Synthesis and Characterization of MEH-PPV for Solar Cell Application. *Egypt. J. Chem.* **59**(5), 911-33 (2016)

2. Yu W.W., Qu L., Guo W., Peng X. Experimental Determination of the Extinction Coefficient of CdTe, CdSe, and CdS Nanocrystals. *Chem. Mater.* **15**(14), 2854-60 (2003).

3. Lee H., Wang M., Chen P., Gamelin D.R., Zakeeruddin S.M., Grätzel M., et al. Efficient CdSe Quantum Dot-Sensitized Solar Cells Prepared by an Improved Successive Ionic Layer Adsorption and Reaction Process. *Nano Lett.* **9**(12), 4221-7 (2009).

4. Mc.Elroy N., Page R.C., Espinbarro-Valazquez D., Lewis E., Haigh S., O'Brien P., et al. Comparison of solar cells sensitised by CdTe/CdSe and CdSe/CdTe core/shell colloidal quantum dots with and without a CdS outer layer. *Thin Solid Films*, **560**, 65-70 (2014).

5. Thambidurai M., Muthukumarasamy N., Agilan S., Murugan N., Vasantha S., Balasundaraprabhu R., et al. Strong quantum confinement effect in nanocrystalline CdS. *J. Mater.Sci.* **45**(12), 3254-8 (2010).

6. Veeraanga M.S.P.K., Ramasamy P., Synthesis and characterization of cadmium sulfide (CdS) quantum dots (QDs) for quantum dot sensitized solar cell applications. *Int. J. Chem. Tech. Res.* **6**, 5396-9 (2014).

7. Bera D., Qian L., Tseng T-K., Holloway P.H. Quantum Dots and Their Multimodal Applications: *A Review. Materials*. **3**(4), (2010).

8. Mattoussi H., Palui G., Na H.B., Luminescent quantum dots as platforms for probing in vitro and in vivo biological processes. *Adv. Drug Delivery Rev.* **64**(2), 138-66 (2012).

9. Birudavolu S., Nuntawong N., Balakrishnan G., Xin Y.C., Huang S., Lee S.C., et al. Selective area growth of InAs quantum dots formed on a patterned GaAs substrate. *Appl. Phys. Lett.* **85**(12), 2337-9 (2004).

10. Nakata Y., Mukai K., Sugawara M., Ohtsubo K., Ishikawa H., Yokoyama N., Molecular beam epitaxial growth of InAs self-assembled quantum dots with light-emission at 1.3μm. *J. Cryst. Growth.* **208**(1), 93-99 (2000).

11. Surana K., Salisu I.T., Mehra R.M., Bhattacharya B. A simple synthesis route of low temperature CdSe-CdS core-shell quantum dots and its application in solar cell. *Opt. Mat.* **82**, 135-40 (2018).

12. Veerathangam K., Pandian M.S., Ramasamy P. Size-dependent photovoltaic performance of cadmium sulfide (CdS) quantum dots for solar cell applications. *J. Alloys Compds.* **735**, 202-8 (2018).

13. Spanhel L., Anderson M.A., Semiconductor clusters in the sol-gel process: quantized aggregation, gelation, and crystal growth in concentrated zinc oxide colloids. *J. Am. Chem. Soc*. **113**(8), 2826-33 (1991).

14. Bera D., Qian L., Sabui S., Santra S., Holloway P.H. Photoluminescence of ZnO quantum dots produced by a sol–gel process. *Opt. Mater.* 30(8); 1233-9 (2008).

15. Qu L., Peng Z.A., Peng X. Alternative Routes toward High Quality CdSe Nanocrystals. *Nano Lett.* **1**(6), 333-7 (2001).

16. Li L., Qian H., Ren J. Rapid synthesis of highly luminescent Cd Tenanocrystals in the aqueous phase by microwave irradiation with controllable temperature. *Chem.Commun.* **4**, 528-30 (2005).

17. Rühle S., Shalom M., Zaban A. Quantum-Dot-Sensitized Solar Cells. *Chem. Phys. Chem.* 11(11), 2290-304 (2010).

18. Pusit P., Sukon P., J. Titanium dioxide powder prepared by a sol - gel method, *Ceram. Process. Res.* **10** (2), 167-70 (2009).

19. Wang M., Hua J., Yang Y., Fabrication of CDs/CdS-TiO_2 ternary nano-composites for photocatalytic degradation of benzene and toluene under visible light irradiation. *Spectrochimica Acta Part A: Molecular and Biomolecular Spectroscopy*. **199**, 102-9 (2018).

20. Zenou V.Y., Bakardjieva S., Microstructural analysis of undoped and moderately Sc-doped TiO_2anatase nanoparticles using Scherrer equation and Debye function analysis. *Mater.Charact.* **144**, 287-96 (2018).

21. Metin H., Esen R., Annealing effects on optical and crystallographic properties of CBD grown CdS films. *Semicond. Sci. Technol.* **18**(7), 647 (2003).

22. Qutub N., Sabir S., Optical, Thermal and Structural Properties of CdS Quantum Dots Synthesized by A Simple Chemical Route. *Int. J. Nanosci. Nanotechnol.* 8(2), 111-20 (2012).

23. Al-Fouadi A.H.A., Hussain D.H., Rahim H.A., Surface topography study of CdS thin film nanostructure synthesized by CBD. *Optik*. **131**, 932-40 (2017).

24. Winter J.O., Gomez N., Gatzert S., Schmidt C.E., Korgel BA., Variation of cadmium sulfide nanoparticle size and photoluminescence intensity with altered aqueous synthesis conditions. *Colloids Surf. A: Physicochemical and Engineering Aspects.* **254**(1), 147-57 (2005).

25. Amany M. El Nahrawy, Ahmed I. Ali, Ali B. Abou Hammad, Aïcha Mbarek, Structural and Optical Properties of Wet-chemistry Cu codoped $ZnTiO_3$ Thin Films Deposited by Spin Coating Method, *Egypt. J. Chem.* **61**(6), 1073 – 81 (2018).

26. Balandin A., Wang K.L., Kouklin N., Bandyopadhyay S., Raman spectroscopy of electrochemically self-assembled CdS quantum dots. *Appl.Phys.lett.* **76**(2), 137-9 (2000).

27. Abdulkhadar M., Thomas B., Study of raman spectra of nanoparticles of CdS and ZnS. *Nanostruct. Mater.* **5**(3), 289-98 (1995).

28. Guo X., Liu C., Exciton-mediated Raman scattering in CdS quantum dot. *Physica E: Low-dimensional Systems and Nanostructures.* **93**, 271-4 (2017).

29. Hossain M.A., Jennings J.R., Koh Z.Y., Wang Q. Carrier Generation and Collection in CdS/CdSe-Sensitized SnO2 Solar Cells Exhibiting Unprecedented Photocurrent Densities. *ACS Nano*. **5**(4), 3172-81 (2011).

30. Shengyuan Y., Nair A. S., Ramakrishna S., Morphology of the electrospun TiO_2 on the photovoltaic properties of CdS quantum dot-sensitized solar cells. *J. Nanosci. Nanotechnol.* **15**(1), 721-5 (2013).

31. Zhang W. D., Chen S., Li X., Wang A. Z., Shi J., Sun Z. et al. Cadmium sulfide quantum dots grown by chemical bath deposition for sensitized solar cell applications. *Proc SPIE.* (2009).

32. Lin S-C., Lee Y-L., Chang C-H., Shen Y-J., Yang Y-M., Quantum-dot-sensitized solar cells: Assembly of CdS-quantum-dots coupling techniques of self-assembled monolayer and chemical bath deposition. *Appl. Phys. Lett.* **90**(14), 143517 (2007).

33. Woo Jung S., Kim J-H., Kim H., Choi C-J., Ahn K-S., CdS quantum dots grown by in situ chemical bath deposition for quantum dot-sensitized solar cells. *J. Appl. Phys.* **110**(4), 044313 (2011).

34. Yu L., Li Z., Liu Y., Cheng F., Sun S., Mn-doped CdS quantum dots sensitized hierarchical TiO_2 flower-rod for solar cell application. *Appl. Surf. Sci.* **305**, 359-65 (2014).

35. Wang B., Ding H., Hu Y., Zhou H., Wang S., Wang T., et al. Power conversion efficiency enhancement of various size CdS quantum dots and dye co-sensitized solar cells. *Int. J. Hydrogen Energy,* **38**(36), 16733-9 (2013).

تأثير النقاط الكمية لكبريتيد الكادميوم المحضرة بواسطة تقنية ترسيب الحمام الكيميائي على أداء الخلايا الشمسية

زينب عبد الحميد[١]، هناء بركات حسن[٢]، منال عبد الرحيم حسن[١]، مجدى محمد حسين[٣]، صفاء أنور[١]
[١]مركز بحوث وتطوير الفلزات - حلوان - القاهرة - مصر.
[٢]كلية العلوم - جامعة القاهرة - الجيزة - مصر.
[٣]المعهد القومي للعلوم المعززة بالليزر - جامعة القاهرة - الجيزة - مصر.

في السنوات الأخيرة أصبحت الطاقة التقليدية إحدي مشاكل العالم وكنتيجة لذلك ازداد الطلب والحاجة إلي مصادر الطاقة المتجدده نظرا لمحدودية الوقود الحفري وقضايا الإحتباس الحراري؛ لذلك فقد برز دور الطاقة الشمسية كمصدر للطاقة المتجددة.

تعتبر الخلايا الشمسية نقاطية الكم احدي انواع الجيل الثالث من الخلايا الشمسية و التي تعتمد علي النقاط الكمية كمواد ممتصة للضوء. النقاط الكمية هي جسيمات أشباه الموصلات بالغة الصغر المستخدمة في الخلايا الشمسية؛ تختلف خصائصها البصرية والإلكترونية عن خصائص الجزيئات الكلية. يمكنهم تحسين أداء الخلايا الشمسية إذا تم تحضيرهم في الحجم المناسب. تمتلك النقاط الكمية عددا من فجوات النطاق (Band Gap) عبر مستويات الطاقة عن طريق تغيير حجم النقط علي عكس المواد الأساسية التي تمتلك فجوات نطاق ثابتة تبعا لنوع الماده المستخدمة. ومن بين الخصائص البارزة للنقاط الكمية أيضا، الطيف الانبعاثي الضيق ، الثبات الضوئي الجيد ، أطياف الإثارة الواسعة، وإرتفاع معامل الاثارة. في هذا العمل، تم تحضير رقائق رقيقة من النقاط الكمية لكبريتيد الكادميوم (CdS) على ركائز أكسيد القصدير المرسبة على الزجاج الموصل الشفاف (FTO). تم تحسين ترسيب Qds QDs باستخدام طريقة ترسيب الحمام الكيميائي في ظل ظروف تشغيل متنوعة (تركيز السلائف، ودرجة الحرارة). هذة الطريقة هى وسيلة فعالة لترسيب CdS على طبقة TiO_2 التي يسهل اختراقها. تم دراسة التركيب و المظهر السطحى (المورفولوجي) والخصائص البصرية للأغشية الرقيقة CdS المعدة باستخدام حيود الأشعة السينية، الميكروسكوب الإلكتروني الماسح، التحليل الطيفي للرامان والأشعة فوق البنفسجية القريبة من الأشعة تحت الحمراء. تم حساب حجم الجسيمات من QDS QDs ليكون 7-3 نانومترى من نمط حيود الأشعة السينية. تحولت فجوة النطاق إلى اللون الأزرق في طيف امتصاص الأشعة فوق البنفسجية مقارنةً f فجوة النطاق الأكبر bulk CdS، مما يؤكد على تشكيل Qds Qds.